Application of entropic approach to estimate the mean flow velocity and Manning roughness coefficient in a high-curvature flume

D. Termini and T. Moramarco

ABSTRACT

The entropy-based approach allows the estimation of the mean flow velocity in open channel flow by using the maximum flow velocity. The linear relationship between the mean velocity, u_{max}, and the mean flow velocity, u_m, through the dimensionless parameter Φ(M), has been verified both in natural rivers and in laboratory channels. Recently, the authors of this study investigated the reliability of the entropy-based formula in a straight channel and under different bed and side-walls' roughness conditions. The present study aims to further validate the entropy-based approach and to explore the effectiveness of entropy-based formula in high curvature channels. Results show that as the effect of the downstream variation of the channel's curvature the value of the parameter Φ(M) varies along the bend. When the bed deformation is evident, the variation of the parameter Φ(M) is strongly reduced compared to that obtained in absence of bed deformation. Results also show that the Manning's roughness coefficients determined through entropy-based formula are in agreement with those estimated by applying other literature's expressions but, unlike the latter, through the parameter Φ(M) the entropy-based formula could account for the effects due to the advective momentum transport by cross-circulation along the strongly curved reaches of the channel.

Key words | discharge, entropy, experiments, monitoring, rivers, simulation

D. Termini (corresponding author)
Dipartimento di Ingegneria Civile, Ambientale e Aerospaziale,
University of Palermo,
Viale delle Scienze,
Palermo 90128,
Italy
E-mail: *donatella.termini@unipa.it*

T. Moramarco
Research Institute for Geo-Hydrological Protection,
CNR,
Perugia,
Italy

INTRODUCTION

The discharge is among the variables most important in the field of hydrological and hydraulic studies (Chiu *et al.* 2005). Indeed, the calibration and validation of models addressed to surface runoff analysis and/or water resource managements can be affected by a wrong estimation of discharge. This may occur mainly for high stages when it is well known that the monitoring of flow velocity is not accurate at all and rating curves often fail (Moramarco *et al.* 2004). However, in the last two decades, many methods have been developed to avoid the problem by leveraging the entropy concept (Chiu 1988) and using the maximum flow velocity, u_{max}, as key variable to estimate the mean flow velocity, u_m (Chiu 1991; Fulton & Ostrowski 2008). Specifically, the entropy model developed by Chiu (1988, 1991) correlates the mean flow velocity to the maximum value using the linear relationship $u_m = \Phi\ (\mathrm{M})u_{\max}$, that depends on the entropic parameter, M (Chiu & Murray 1992). Xia (1997) verified this relationship in some sections of the Mississippi River and found that it is perfectly linear both along the straight and the curved channel reaches, obtaining M values quite similar for sections located along straight branches and equal to 2.1; whereas for sites along bends the M value was equal to 4.8. Similar findings were obtained by other studies investigating a number of gauged sections located in different rivers (Ammari & Remini 2010; Moramarco & Singh 2010; Farina *et al.* 2014, to cite a few). Therefore, if one knows the value of M and the maximum velocity, the cross-sectional mean velocity can be estimated

doi: 10.2166/nh.2016.106

and, as a consequence, the discharge given the river cross-section geometry. This insight explains the interest that drove Moramarco & Singh (2010) to investigate the dependence of the entropic parameter M on the hydraulic and geometric characteristics of the river cross section. They inferred that the constant value of M can be justified on the ground that it is found not to depend on the flood dynamic, as expressed by the energy or water surface slope S_f. This remarkable concept allowed them to derive a 'new' formulation for the roughness estimation based on the entropy parameter M and where the location y_o, for which the velocity is assumed equal to zero, had an important role distinguishing low flows from the high ones. Afterwards, Moramarco & Termini (2015) investigated the reliability of the roughness entropy formula along with the sensitivity of the roughness formula on y_o on the basis of experimental data collected in straight laboratory flumes under different bed (including the presence of vegetation) and side-wall roughness conditions. The main finding of this study was that the roughness entropy formula is quite robust to represent the observed flow resistance also in the presence of vegetation.

The purpose of the present study is, therefore, to further validate the linear relationship $u_m = \Phi\ (M)\ u_{max}$ and to extend the analysis on the effectiveness of roughness entropy formula in high curvature channels. The analysis is conducted on the basis of experimental data collected in a meandering flume constructed at the Dipartimento di Ingegneria Civile, Ambientale, Aerospaziale e dei Materiali (DICAM – University of Palermo, Italy), for different bed configurations, and in particular, for rigid flat-bed and fixed-deformed bed conditions.

The paper is organized as follows: the next section describes the experimental dataset followed by a section illustrating and discussing the experimental results. Finally, conclusions are drawn in the last section.

DATA AND METHODS

Experimental data

The data set used in the present work was collected in the ambit of previous studies aimed to analyze the flow pattern along a high-curvature meandering channel. Thus, details of the experimental setup and measurement conditions can be found in previous works (see e.g., Termini 2009; Termini & Piraino 2011) and only features of particular interest for the analysis presented in this work are briefly summarized here.

The channel follows the sine-generated curve with a deflection angle at the inflection section $\theta o = 110^{\circ}$. The channel cross section was rectangular with width $B = 0.50$ m; the fixed vertical sidewalls were of plexiglass and the bed was of quartz sand (d_{50} = medium sediment diameter = 0.65 mm, σ_g = geometric standard deviation = 1.34). The meandering channel was 25.12 m long in order to accommodate two meander wavelengths; the upstream and downstream ends of the meandering channel were connected to two straight channels of 3 m and 2 m long, respectively.

Two runs were carried out with initial flow discharge $Q = 0.012\ m^3/s$, longitudinal centerline bed slope S = 0.371%, initial channel-averaged flow depth h = 5.2 cm ($B/h = 9.09 < 10$, $R_{min}/B = 1.94$, with R_{min} = radius of curvature at centerline of the apex section). The first run was conducted over the rigid flat-bed (herein called the FB run) in order to analyze the effect of channel's curvature neglecting the effect of the bed deformation. Then a mobile-bed run was conducted with the same initial hydraulic conditions as those of the FB run. In this case, the channel-averaged flow depth was identified with the flow depth at the centerline of the channel's crossovers (control sections). After that the equilibrium bed configuration was reached, the deformed sand bed was fixed by cement dust and spray paint (see Termini & Piraino 2011) and another run (herein called the DB run) was conducted over the fixed-deformed bed in order to measure the flow velocity components. During the DB run, the marks of flow meters located at the control sections were used to check the reaching of the same hydraulic conditions as the previous mobile-bed run.

During each run, the water and bed surfaces were measured using a Profiler Indicator PV09 (Delft Hydraulics) with precision of 0.1 mm. The instantaneous velocity components were measured in cross sections spaced about 50 cm or so apart, starting from section 1 (see Figure 1). In this work, the analysis is restricted to sections indicated in Figure 1 which are selected along the channel reach

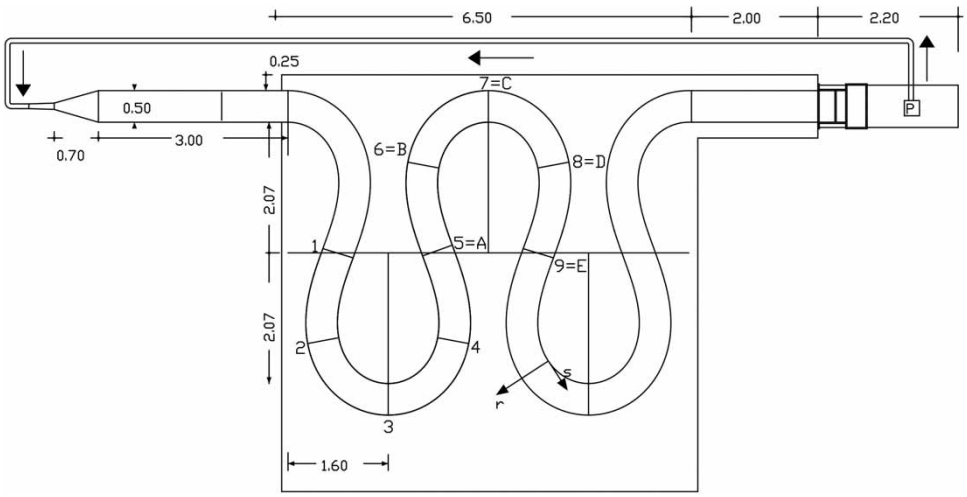

Figure 1 | Experimental apparatus.

between two consecutive inflection sections. During the FB run, the instantaneous longitudinal, $u(t)$, and transversal, $v(t)$, velocity components were measured by using a 2D side-looking Acoustic Doppler Velocimeter (ADV) manufactured by SonTek Inc., in points spaced 1–1.5 mm along the verticals of nine transverse abscissas symmetrically to the channel axis (see details in Termini 2009)). During the DB run, the ADV did not provide accurate measured data near the inner bank of each bend, where point bars developed and small water depths occurred and thus the Ultrasonic Doppler Velocimeter (DOP2000) manufactured by Signal Processing SA was used. The instantaneous longitudinal, $u(t)$, transversal, $v(t)$, and vertical, w(t), velocity components were measured by using a probe of 4 Mhz. The distance between the centers of adjacent sampling volumes was 0.75 mm (see details in Termini & Piraino 2011).

Pertinent aspects of friction factor estimation and summary of previous results

Before proceeding further, it seems important to briefly summarize here peculiar findings in the literature regarding friction factor estimation in meandering streams and recent results in estimating the roughness coefficient by applying the entropy-based formula.

(i) In most works on meandering streams (among others, Nelson & Smith 1989; Chu *et al.* 1991) the dimensionless Chèzy friction factor c is considered constant and invariably identified by using relations formulated for straight channels as (see Yalin 1992):

$$c = \text{with } A_s = e^{\kappa B_s - 1} \tag{1}$$

$$\bar{c} = \frac{1}{\kappa}\ln\left(A_s \frac{h}{k_s}\right)$$

where $\kappa =$ Von Karman constant, $k_s =$ effective bed roughness, $B_s =$ coefficient that depends on the flow regime – see Yalin (1992, p. 10). However, from the literature it is also clear that the resistance to flow can be significantly increased because of the bed deformation and/or the channel's curvature (see e.g., Onishi *et al.* 1976; Steffler *et al.* 1985; James 1994; Khan & Steffler 1996). In fact, since in meandering channels the flow characteristics vary from one location in the flow plan to another, the friction factor also should vary depending on location (Da Silva 1999). Various methods have been proposed in the literature for accounting the additional resistance in curved channel reaches. Onishi *et al.* (1976) argued that the difference between the friction factors for meandering and straight channel flows, $(c - \bar{c})$, is a function of three dimensionless parameters: the Froude number, the relative roughness R_h/d_{50} ($R_h =$ hydraulic radius), and the ratio B/R ($R =$ radius of curvature of channel axis). In particular, Onishi *et al.* (1976)

established that the head loss due just to the bend, normalized by the mean velocity, essentially tends to increase with the aforementioned dimensionless parameters. In order to include the bend's effect in depth-averaged solving momentum equations, Johannesson & Parker (1984) suggested including additional terms depending on the bed friction coefficient. Da Silva (1999) analyzed the variability of the friction factor in meandering streams. By applying the dimensional analysis and using data collected in two sine-generated meandering laboratory channels, respectively characterized by low (deflection angle at inflection section $\theta_o = 30^\circ$) and high (deflection angle at inflection section $\theta_o = 110^\circ$) amplitude, Da Silva (1999) revealed that in a wide meandering stream, and for a given relative roughness, the value of the friction factor varies along the channel as a function of the ratio B/R, the channel's curvature and sinuosity (identified in a sine-generated curve by θ_o). With the aid of data collected in flat-bed condition and in the same meandering laboratory channel as that of Figure 1, Termini (2002) related the difference between the friction factors for meandering and straight channel flows to typical control parameters for curved flows (see, among others, Blanckaert & de Vriend 2010; Termini 2015a, 2015b) which are the ratios parameters B/R and r/R (r = local radius of channel's curvature).

(ii) Moramarco & Singh (2010) verified that in open channel flow the roughness coefficient can be related to the entropic parameter M by the following expression:

$$n = \frac{R_h^{1/6}/\sqrt{g}}{\Phi(M)\frac{1}{k}\left[\ln\left(\frac{y_{\max}}{y_o}\right) + \frac{D}{y_{\max}}\ln\left(\frac{D}{h}\right)\right]} \quad (2)$$

where n = Manning's roughness coefficient, y_{max} = location from the bed where the maximum velocity occurs, D = location of maximum velocity, u_{max}, below the water surface, y_o = location where the logarithm profile predicts the zero velocity. It should be clear from the 'Introduction' that y_o is a parameter of Equation (2) which has to be adequately calibrated by using experimental data. Moramarco & Termini (2015), by using a data set collected in straight laboratory flumes, verified the applicability of the linear entropic relationship $u_m = \Phi(\mathrm{M})\ u_{max}$, for different roughness conditions of the bed and the side walls. In particular, they examined three roughness conditions of the walls: (a) rough bed and smooth side-walls; (b) rough bed and side-walls; (c) vegetated bed and smooth side-walls. The results obtained by Moramarco & Termini (2015) showed that for all the examined roughness conditions, and including vegetated-bed condition but with high values of flow submergence (i.e., $h/k_v > 2$, with k_v = bent vegetation height) and low values of stems concentration, the ratios $u_m/u_{max} = \Phi(\mathrm{M})$ fall inside the range 0.5–0.8 arranging around a mean value $\Phi(\mathrm{M}) = 0.64$ that is quite similar to that identified in many natural rivers (see, e.g., Moramarco & Singh 2010). In vegetated-bed condition and for low values of flow submergence (i.e., $h/k_v < 2$) and high stems' concentration, the ratios $u_m/u_{max} = \Phi(\mathrm{M})$ arrange around a mean value of about 0.3. According to Moramarco & Termini (2015), such a different behavior is essentially due to the difference in the mechanism of the momentum exchange for high flow submergence and low flow submergence conditions (Termini 2015b). In fact, as highlighted by Termini (2015b) (see also Carollo *et al.* 2008), unlike the case of high flow submergence, for low flow submergence the vertical velocity profile can be schematized into two layers (i.e., inside and outside the vegetation layer) of almost constant velocity which is separated by a very thin band where the momentum exchange occurs. Thus, Moramarco & Termini (2015) verified that Equation (2) is quite robust to represent the flow resistance also in the presence of vegetation, regardless of the stems' concentration, although for $h/k_v < 2$ a sort of 'boundary zone' is identified and high and variable n-values are obtained.

EXPERIMENTAL RESULTS

Estimation of mean velocity and entropic relation u_{max}-u_m

In order to validate the linear relationship $u_m = \Phi(\mathrm{M})\ u_{max}$ for the meandering stream, the maximum value of

longitudinal velocity, $u_{max,v}$, along with flow depth has been identified for each measurement vertical of each run. Then, the integration of these vertical profiles also allowed the identification of the vertical mean velocity, $u_{m,v}$. Figure 2 shows, for each run, the comparison between the values of $u_{max,v}$ with the values of $u_{m,v}$. From Figure 2 it can be observed that the pairs of values ($u_{max,v}$, $u_{m,v}$) could be interpolated by a linear equation for both runs. For the FB run the points are very well interpolated and the coefficient R^2 assumes a value of 0.95; for the DB run the points are more dispersed and the coefficient R^2 assumes a value of around 0.54. The different behavior observed in the examined conditions could be due to the fact that while in the FB run the flow pattern is only affected by the downstream changing of the channel's curvature, in the DB run the combined effect of the channel's curvature and the bed topography modifies the evolution of the cross-sectional flow and the momentum transport related to it. Studies (see, e.g., Blanckaert & Graf 2004; Termini 2015a) have demonstrated that the advective momentum transport by cross-circulation exerts an important role in the downstream velocity redistribution along the channel. In particular, Termini (2015a), by using the same data set as that in the DB run, verified that the advective momentum transport by cross-circulation varies along the meandering bend: it increases passing from the inflection section upstream (section A of Figure 1) to the bed entrance (section B of Figure 1) so that the core of high velocities is found at a certain distance from the outer bank; at the apex section (section C of Figure 1), the core of high values shifts towards the centerline until that at the bend exit (section E of Figure 1) is found at the centerline. This is because, as shown in Termini & Piraino (2011), a counter-rotating circulation cell is initiated in the upper part of the outer-bank of the bend entrance (section B of Figure 1), it is fully developed at the bend apex (section C of Figure 1), and then it disappears at the bend exit (section D of Figure 1). Thus, along the channel reach of higher curvature (sections B, C, D), the presence of the counter-rotating circulation cell: (i) modifies the advective momentum transport by cross-circulation (Termini 2015a), (ii) attenuates the action of the central-region circulation cell, and (iii) maintains the core of high velocities at a certain distance from the outer bank (Termini & Piraino 2011).

Bearing this behavior in mind, the pairs ($u_{max,v}$, $u_{m,v}$) estimated for the DB run at the measurement vertical close to the outer bank in sections B, C, and D were neglected and the remaining pairs of values ($u_{max,v}$, $u_{m,v}$) have been interpolated again (see Figure 3). It can be seen from Figure 3 that the points are better interpolated than in Figure 2(b), obtaining a coefficient R^2 around 0.69. This confirms that the advective momentum transport by cross-circulation strongly affects the distribution of the downstream flow velocity along the channel and, in turn, the value of the mean value $u_{m,v}$ at each measurement vertical.

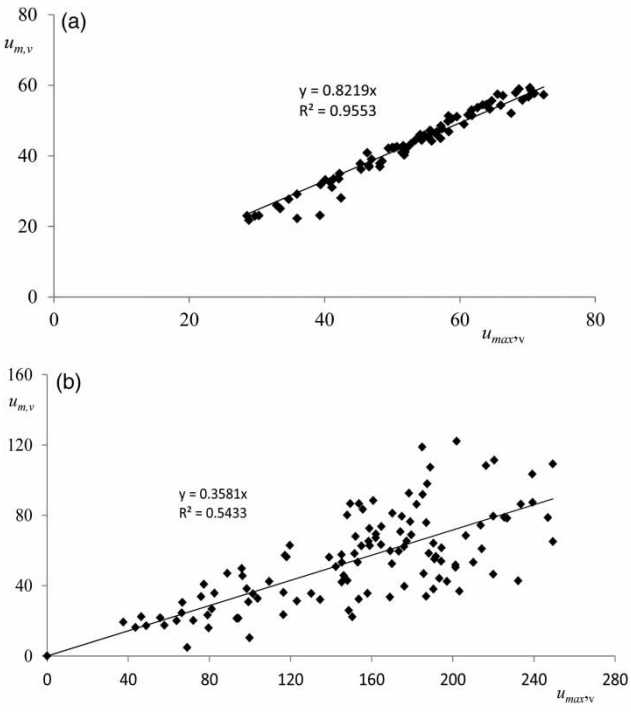

Figure 2 | Relation between $u_{max,v}$ and $u_{m,v}$: (a) FB run; (b) DB run.

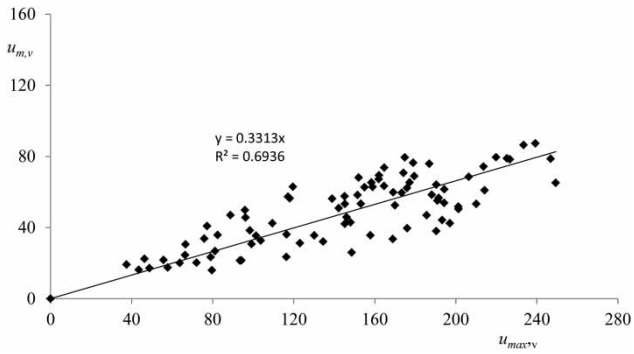

Figure 3 | Relation between $u_{max,v}$ and $u_{m,v}$: DB run by excluding measurement vertically close to the outer bank in sections B, C, and D.

Then, for each run, the measured profiles were integrated on the entire cross section and the cross-sectional mean velocity, u_m, has been determined. Thus, the ratios between the cross-sectional mean velocity and maximum cross-sectional flow velocity, u_{max}, have been estimated. Figure 4 reports, for both runs, the box-plots of the ratios u_m/u_{max}. In this figure the central rectangle spans the first quartile to the third quartile ('interquartile range'), the triangle inside the rectangle shows the median value of the distribution, and the extreme points above and below the box show the locations of the minimum and maximum. From Figure 4 it can be observed that in the FB run the median value is equal to about 0.64, in agreement with studies conducted in natural rivers (see, e.g., Moramarco & Singh 2010), while in the DB run the median value is equal to about 0.25. As it should be clear from the sub-section 'Pertinent aspects of friction factor estimation and summary of previous results', the median value of the ratio u_m/u_{max} obtained in the DB run is close to that previously obtained by Moramarco & Termini (2015) in vegetated-bed condition for low flow submergence and high stems' concentration. Such a similarity suggests that the modified zone of momentum exchange and the modified distribution of the downstream velocity profile determine a different (lower) value of the parameter Φ(M).

Figure 4 also shows that the interquartile range obtained in the FB run is higher than that obtained in the DB run and, thus, the dispersion of the distribution in the FB run is higher than that in the DB run. Furthermore, for both runs, the distribution is not symmetrical, but in the DB run the box-plot is smaller than in the FB run. This means that, overall, the values of the ratios u_m/u_{max} estimated for the DB run have a high level of agreement with each other while those estimated for the FB run are more variable along the bend. The variability of the ratios u_m/u_{max} observed in the FB could be related to the flow pattern which is only affected by the downstream variation of the channel's curvature. In such a case, in fact, Termini (2009) observed that the core of high velocities gradually shifts from the inner bank at the inflection section upstream (section A of Figure 1) to the outer bank at the inflection section downstream (section E of Figure 1). Thus, the flow accelerates along the outer bank and decelerates along the inner bank so that the highest values of the longitudinal velocity are obtained at the inflection sections. Consequently, the value of the ratio u_m/u_{max} varies as one passes from the inflection section to the apex section along the bend.

In field applications, the mean velocity, $U = Q/(Bh)$, is usually considered as the most important hydraulic variable and, thus, the ratios U/u_{max} have also been estimated for each run. In Figure 5 the ratios u_m/u_{max} are plotted against

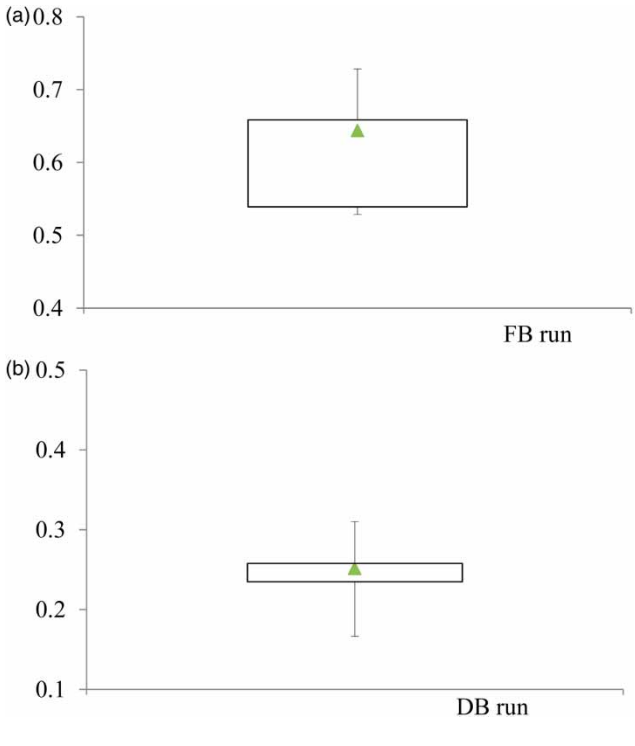

Figure 4 | Box plot ratios u_m/u_{max}: (a) FB run; (b) DB run.

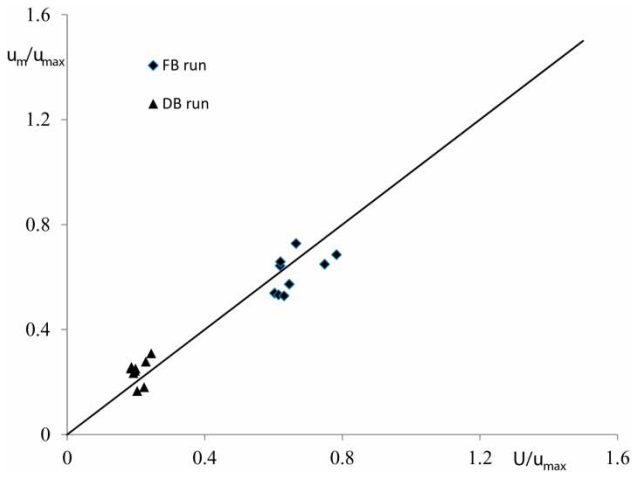

Figure 5 | Comparison between the ratios u_m/u_{max} and the ratios U/u_{max}.

the ratios U/u_{max}. As Figure 5 shows, the points thicken around the bisecting line thus demonstrating that the values of u_m obtained from the experimental profiles well approximate the cross-sectional mean velocity U. Consequently, the ratios U/u_{max} have been examined, and in Figure 6 the values of U/u_{max} estimated in sections A–E for each run have been compared. For the DB run also the values of U/u_{max} determined along the upstream bend (i.e., in sections $1 \div 5$ of Figure 1) were reported. From Figure 6 it can be observed that, for both runs, the ratio U/u_{max} increases passing from the inflection section (section A) to the apex section (section C) where the maximum value is obtained; then, as the channel's curvature decreases, the ratio U/u_{max} decreases again until it reaches the inflection section downstream (section E). This is more accentuated in the FB run than in the DB run. In particular, it can be seen that in the FB run a value of $U/u_{max} \cong 0.8$ is obtained approximately at the apex section and a value of $U/u_{max} \cong 0.6$ is obtained at the inflection sections. It is worth noting this behavior is consistent with results obtained by Xia (1997) investigating the ratio U/u_{max} in the Mississippi River. Xia (1997) obtained a value of the ratio U/u_{max} of around 0.8 in curved reaches ($R/B =$ ranging from 1.1 and 7.7, with $R =$ local centerline radius of curvature) and of around 0.68 in straight reaches. He attributed such a variation of the ratio U/u_{max} to the fact that, for the same cross-sectional mean flow U, the magnitude of u_{max} on the straight reaches was greater than that on the bends. As mentioned above, in the FB run a behavior similar to that observed by Xia (1997) can be seen. In fact, in this case, passing from the inflection section to the apex section the flow accelerates along the outer bank and decelerates along the inner bank so that the highest values of u_{max} are found at the inflection sections A and E. In contrast to this, in the DB run, the difference in magnitude of u_{max} at the inflection sections and at the apex section is not very accentuated. Thus, the difference between the values of the ratios U/u_{max} obtained in the DB run, in the inflection section and in the apex section is reduced compared to that obtained in the FB run. As previously mentioned, this is due to the fact that, according to Termini (2009), in the DB run the point bar developing near the inner bank forces the flow towards the opposite bank and enhances the convective pattern of flow so that, passing from the inflection section (section A of Figure 1) to the bend entrance (section B of Figure 1), the core of high velocities shifts immediately towards the outer bank region. In this section, as mentioned before, Termini & Piraino (2011) and also Termini (2015a, 2015b) observed that, besides the main central-region circulation cell, a counter-rotating circulation cell initiates in the upper part of the outer bank region so that the core of high velocities is maintained at a certain distance from the outer bank. This behavior is maintained until the bend exit is reached (section D of Figure 1). Thus, in this case, although the bed deformation tends to enhance the flow convective pattern, the cross-sectional motion attenuates it (Termini & Piraino 2011).

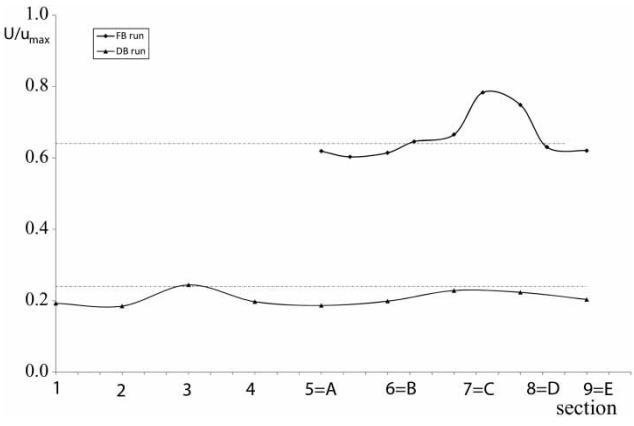

Figure 6 | Ratios U/u_{max}.

Manning's roughness coefficient

Based on the results shown in the sub-section 'Estimation of mean velocity and entropic relation u_{max}-u_m', attention is now focused on the validation of the entropy-based formula, Equation (2), in a high-amplitude meandering flume. In accordance with Moramarco & Termini (2015), the analysis is performed by the comparison of the Manning's roughness coefficient, n, estimated by Equation (2) with those estimated both by applying empirical formulas found in the literature and by applying the classical Manning formula, written as follows:

$$n = \frac{R_h^{1/6}/\sqrt{g}}{u_m/u_*} \tag{3}$$

where R_h = hydraulic radius, u_* = shear velocity estimated by using the measured data and the law of the wall (see Whiting & Dietrich 1990; Termini 2002). In accordance with Moramarco & Termini (2015), hereafter the n-values estimated by Equation (3) are called 'observed' n-values.

As mentioned in the sub-section 'Pertinent aspects of friction factor estimation and summary of previous results', Da Silva (1999) analyzed the variation of friction factor by using collected in sine-generated meandering laboratory channels, for two values of the deflection angle at inflection section ($\theta_o = 30^\circ, 110^\circ$) and in flat-bed condition. As a result, the following expression to estimate the local friction factor, c, was proposed:

$$\left[\left(\frac{\bar{c}}{c}\right)^2 - 1\right] = \varphi(\theta_o)\left[\left(\left(\frac{R}{r}\right)^2 - 1\right) - \left(4\left(\frac{R}{B}\right)^2 - 1\right)^{-1}\right] \quad (4)$$

where r is the local radius of curvature, $\bar{c}$ indicates the friction factor for straight channels estimated by Equation (1), $\varphi(\theta_o)$ is a function that has to be determined by using measured data. Da Silva (1999) suggested the value $\varphi(\theta_o) = 0.17$ for $\theta_o = 30^\circ$ and the values $\varphi(\theta_o) = 1.7$ for $\theta_o = 110^\circ$.

Termini (2002), with the aid of data collected with a flat bed in the same meandering laboratory channel as that of Figure 1, related the normalized difference between the friction factors for meandering and straight channel flows to the parameters r/R and B/R as follows:

$$\frac{c - \bar{c}}{\bar{c}} = a_1\frac{r}{R} + a_2\frac{B}{R} + a_3 \quad (5)$$

where a_1, a_2, a_3 are coefficients which have to be estimated using experimental data. For the considered case ($\theta_o = 110^\circ$), Termini (2002) suggested the values: $a_1 = 0.125756$, $a_2 = -0.00994$, $a_3 = -0.12482$.

On the basis of Equation (5), the difference between the friction factors for meandering and straight channel flows is related to control parameters for curved flows: the ratio r/R accounts for the local curvature effect and the parameter R/B accounts for high-curvature effects; the coefficient a_3 identifies the value of the normalized difference $(c - \bar{c})/\bar{c}$ along the almost straight channel reach (i.e., at the crossovers), where $1/R \cong 0$. According to Equation (5), the difference increases as the channel axis curvature ($1/R$) increases and, thus, passing from the inflection section to the apex section. Moreover, in each cross section (i.e., for a given $1/R$), the normalized difference $(c - \bar{c})/\bar{c}$ increases as the local radius r increases assuming the highest value at the outer bank. This is in agreement with previous works (Yalin & Silva 2001) which indicate that the friction factor increases progressively with r.

Thus, in order to validate Equation (2), the values of the friction factor c have been also estimated by using Equations (4) and (5) and the Manning's roughness coefficient, n, has been determined as follows:

$$n = \frac{R_h^{1/6}}{(c\sqrt{g})} \quad (6)$$

In accordance with Moramarco & Termini (2015), in Equation (2), the variable y_o has been linked to the median sediment diameter, d_{50} (see also Yalin 1992) and it has been assumed $y_o = k_s = 2d_{50}$.

The comparison between the 'observed' n-values, determined for both runs by Equation (3), and the 'estimated' ones, respectively by Equations (2), (4), and (5), in the FB run and in the DB run conditions are reported in Figure 7. It can be seen that in the FB condition (Figure 7(a)), the values of Manning's roughness coefficient estimated by Equation (2) compare very well with the observed ones; the comparison with the n-values estimated by Equation (5) is also good, although Equation (5) slightly underestimates the n-values for lower water depths. On the contrary, the n-values determined by Equation (4) vary inside a wide range of overestimation, especially for higher water depths, the n-values compared with those estimated both by using Equations (3) and (5). This is also consistent with results previously obtained by Termini (2002) comparing the c-values determined by Equations (4) and (5) under hydraulic conditions different from those considered in the present work.

In Figure 7(b), the comparison between the n-values obtained by applying Equation (2) and those estimated by Equations (3)–(5) in deformed-bed condition (DB run) is shown. In this figure, the n-values estimated by Equation

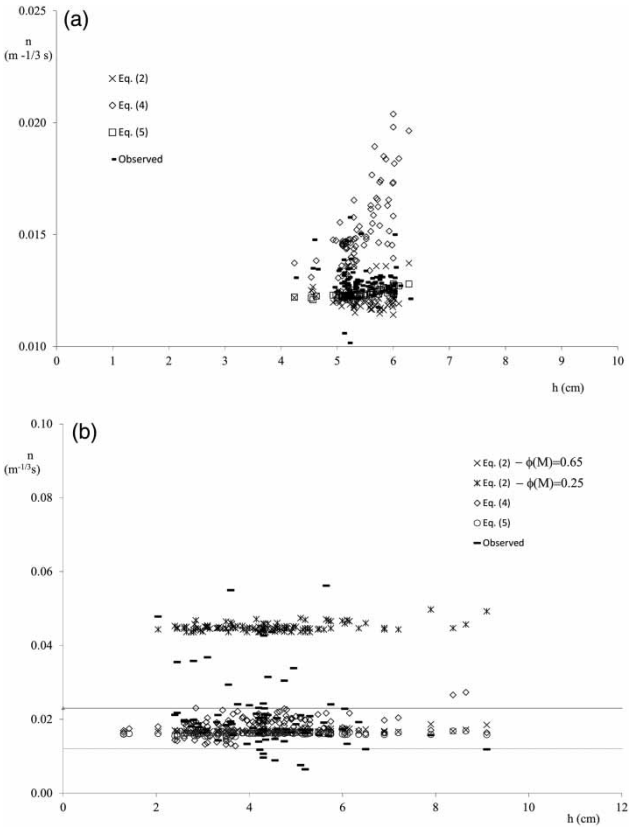

Figure 7 | Comparison between observed *n*-values and estimated ones by Equations (2), (4) and (5): (a) FB run; (b) DB run.

(2), both by assuming $\Phi(M) = 0.64$ (that is the median value of the ratios u_m/u_{max} distribution obtained in flat-bed condition – see Figure 4) and by assuming $\Phi(M) = 0.25$ (that is the median value of the ratios u_m/u_{max} distribution obtained in deformed-bed condition – see Figure 4) are reported. It can be seen that the major part of both the observed *n*-values and those estimated by Equations (4) and (5) fall in the range 0.013–0.023. The *n*-values determined by using Equation (2) with $\Phi(M) = 0.64$ fall inside the aforementioned range and are well comparable with those estimated by applying Equation (5). It should be noted that the observed *n*-values greater than the superior limit of the aforementioned range (called 'out points') refer to radial abscissas corresponding to the measurement verticals close to the outer bank in sections B, C, and D, where the effect of the counter-rotating circulation cell is evident, as described in the sub-section 'Estimation of mean velocity and entropic relation u_{max}-u_m'. These 'out points' fall inside a range which includes the *n*-values estimated by Equation (2) with $\Phi(M) = 0.25$. This further confirms that the advective momentum transport by cross-circulation exerts a significant role on the downstream velocity distribution along the channel, modifying the vertical profiles and, thus, the shear velocity distribution.

Thus, it can be concluded that the entropy-based formula, Equation (2), with $\Phi(M) = 0.64$, is generally in agreement with those estimated by applying the literature expressions formulated in flat-bed condition, but it does not allow accounting for the effects related to the variation of advective momentum transport by cross-circulation occurring at the outer-bank region along the strongly curved reaches of the channel observed in previous studies (Blanckaert & Graf 2004; Termini 2015a, 2015b). Indeed, to reproduce the correct Manning value at the outer bank side, it is necessary to consider a different value of $\Phi(M) = 0.25$ which is always given from the ratio of u_m/u_{max} in that region. This means that the cross-circulation cell changes significantly the velocity profile shape moving the location of u_{max} much more below the water surface (dip) and creating at once a reduction of Manning value. Therefore, this phenomenon tied to secondary currents' effects can be taken into account from the entropy theory able to modify the profile according to the $\Phi(M)$ parameter and, consequently, the Manning value given by Equation (2).

Finally, for both runs, the good fit between the observed *n*-values and those estimated by Equations (2), (4) and (5) has been verified and is shown in Figure 8. Inspecting Figure 8(a), it can be seen that for the FB run, with the exception of some points, Equation (2) (with $\Phi(M) = 0.64$) performs favorably in the range of the observed values. In the DB run (see Figure 8(b)), the variability of the observed *n*-values due to the variation of the momentum transport by cross-circulation along the bend is not cached especially by using Equations (4) and (5) while the higher observed *n*-values are well approximated by Equation (2) with $\Phi(M) = 0.25$. This further confirms that, as mentioned, the effects due to the advective momentum transport by cross-circulation along the strongly curved reaches should be correctly taken into account by the variation of the $\Phi(M)$ parameter in Equation (2). This finding deserves more investigation and will be the object of a future study.

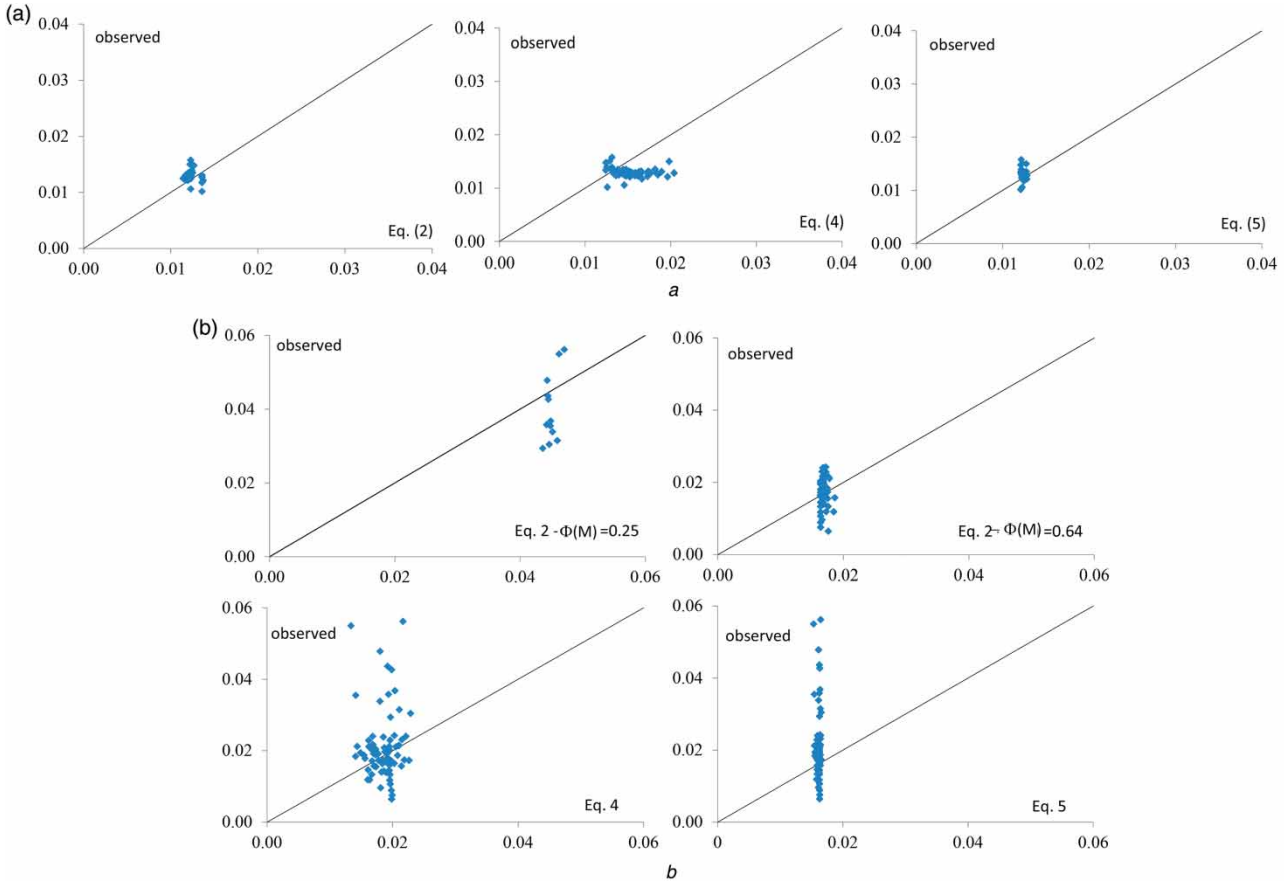

Figure 8 | Comparison between the 'observed' *n*-values and those estimated by Equations (2), (4) and (5): (a) FB run; (b) DB run.

CONCLUSION

This paper presents a study on the applicability of the entropic approach in high curvature channels. In particular, attention is focused on the validation of the linear relationship $u_m = \Phi(M)\, u_{max}$ and on effectiveness of the entropy-based formula to estimate Manning's roughness coefficient in a high-amplitude meandering bend. The main results of the present study can be summarized as follows:

(i) As effect of the downstream variation of the channel's curvature, the value of the parameter Φ(M) varies along the bend. In particular, it increases passing from the inflection section to the apex section and decreases from the apex section to the inflection section downstream. Such a variation is more accentuated when the effect of the bed deformation, compared to that of the channel's curvature, is neglected. In this case, values of the parameter Φ(M) of around 0.8 and 0.6 have been obtained at the apex section and at the inflection section, respectively. This result is consistent with results previously obtained by Xia (1997), investigating the ratio between the cross-sectional mean velocity, U, and the maximum one, u_{max}, in the Mississippi River. According to Xia (1997), such a variation of the Φ(M) parameter is related to the fact that, for the same cross-sectional mean flow U, the magnitude of u_{max} on the almost straight reaches is greater than that on the strongly curved reaches, as previously verified by Termini (2009) in the same meandering channel as that considered in the present work.

(ii) When the effect of the bed deformation cannot be neglected, the variation of the parameter Φ(M) along the bend is strongly reduced compared to that obtained in the absence of bed deformation. This is due to the fact that the bed deformation tends to enhance the flow

convective pattern but such a convective pattern is attenuated by the cross-sectional motion. Thus, the combined effect of the channel's curvature and bed topography on the cross-sectional momentum transport along the bend determines that the difference in magnitude of u_{max} on the inflection section and on the apex section is not very accentuated. This is consistent with previous results obtained on the evolution of the cross-sectional flow along the meandering bend by Termini & Piraino (2011) – see also Termini (2015a).

(iii) When the effect of the bed deformation is neglected, the values of the Manning's roughness coefficients determined by applying the entropy-based formula compare very well with those estimated by using the classical Manning's equation and the expression formulated by Termini (2002) for meandering bends and flat-bed condition. When the effect of the bed deformation is considered, the Manning's roughness coefficients determined by applying the entropy-based formula are generally in agreement with those estimated by applying the aforementioned expressions (formulated in flat-bed condition), but this does not allow accounting for the effects due to the variation of the advective momentum transport by cross-circulation occurring at the outer bank region along the strongly curved reaches of the channel. This result further confirms previous literature findings (Blanckaert & Graf 2004; Termini 2015a) which indicate that the advective momentum transport by cross-circulation exerts a significant role on downstream velocity redistribution, modifying the vertical profiles and the shear velocity distribution along the channel. In order to take the advective momentum transport into account for the bed deformation, the correct parameter of Φ(M) has to be envisaged and which reflects the modified velocity profiles in the outer-bank region. This finding deserves more investigation and will be the object of a future study.

REFERENCES

Ammari, A. & Remini, B. 2010 Estimation of Algerian rivers discharges based on Chiu's equation. *Arabian Journal of Geosciences* **3**, 59–65. doi: 10.1007/s12517-009-0056-y.

Blanckaert, K. & de Vriend, H. J. 2010 Meander dynamics: a nonlinear model without curvature restrictions for flow in open-channel bends. *Journal of Geophysical Research* **115** (F4), 1–22. doi: 10.1029/2009JF001301.

Blanckaert, K. & Graf, W. H. 2004 Momentum transport in sharp open-channel bends. *Journal of Hydraulic Engineering* **130** (3), 186–198.

Carollo, F., Ferro, V. & Termini, D. 2008 Flow velocity profile and turbulence characteristics in a vegetated straight flume. In: *International Congress Riverflow 2008, Cesnme, Izmir, Turkey*, 3–5 September.

Chiu, C. L. 1988 Entropy and 2-D velocity distribution in open channels. *Journal of Hydraulic Engineering* **114** (7), 738–756.

Chiu, C. L. 1991 Application of entropy concept in open-channel flow study. *Journal of Hydraulic Engineering* **117** (5), 615–628.

Chiu, C. L. & Murray, D. W. 1992 Variation of velocity distribution along non-uniform open-channel flow. *Journal of Hydraulic Engineering* **118** (7), 989–1001.

Chiu, C. L., Hsu, S.-M. & Tung, N.-C. 2005 Efficient methods of discharge measurements in rivers and streams based on the probability concept. *Hydrological Processes* **19**, 3935–3946. doi: 10.1002/hyp.5857.

Chu, V. H., Wu, J. H. & Khayat, R. E. 1991 Stability of transverse shear flows in shallow open channels. *Journal of Hydraulic Engineering* **117** (10), 1370–1388.

Da Silva, A. M. 1999 Friction factor of meandering flows. *Journal of Hydraulic Engineering* **125** (7), 779–783.

Farina, G., Alvisi, S., Franchini, M. & Moramarco, T. 2014 Three methods for estimating the entropy parameter M based on a decreasing number of velocity measurements in a river cross-section. *Entropy* **16**, 2512–2529. doi:10.3390/e16052512.

Fulton, J. & Ostrowski, J. 2008 Measuring real-time streamflow using emerging technologies: radar hydroacoustics and the probability concepts. *Journal of Hydrology* **357**, 1–10.

James, C. S. 1994 Evaluation of methods for predicting bend loss in meandering channels. *Journal of Hydraulic Engineering* **120** (2), 245–253.

Johannesson, H. & Parker, G. 1989 Velocity redistribution in meandering rivers. *Journal of Hydraulic Engineering* **115** (8), 1019–1039.

Khan, A. A. & Steffler, P. M. 1996 Vertically averaged and moment equations model for flow over curved beds. *Journal of Hydraulic Engineering* **122** (1), 3–9.

Moramarco, T. & Singh, V. P. 2010 Formulation of the entropy parameter based on hydraulic and geometric characteristics of river cross sections. *Journal of Hydrologic Engineering* **15** (10), 852–858. doi:10.1061/(ASCE)HE.1943-5584.0000255.

Moramarco, T. & Termini, D. 2015 Entropic approach to estimate the mean flow velocity: experimental investigation in laboratory flumes. *Environmental Fluid Mechanics* **15** (6), 1163–1179.

Moramarco, T., Saltalippi, C. & Singh, V. P. 2004 Estimation of mean velocity in natural channel based on Chiu's velocity distribution equation. *Journal of Hydrologic Engineering* **9** (1), 42–50.

Nelson, J. M. & Smith, D. 1989 Evolution and stability of erodible channel beds. In: *River Meandering* (S. Ikeda & G. Parker,

eds). American Geophysical Union, Washington, DC, USA, pp. 321–377.

Onishi, Y., Jain, S. C. & Kennedy, J. F. 1976 Effects of meandering in alluvial streams. *Journal of Hydraulic Division* **102** (7), 899–918.

Steffler, P. M., Rajaratnam, N. & Peterson, A. W. 1985 Water surface at change of channel curvature. *Journal of Hydraulic Engineering* **111** (5), 866–870.

Termini, D. 2002 Friction factor variation in a meandering channel. In: *2nd International Conference: New Trends in Water and Environmental Engineering for Safety and Life: Eco-compatible Solutions for Aquatic Environments*, *Capri, Italy*, June 24–28.

Termini, D. 2009 Experimental observations of flow and bed processes in a large-amplitude meandering flume. *Journal of Hydraulic Engineering* **135** (7), 575–587.

Termini, D. 2015a Momentum transport and bed shear stress distribution in a meandering bend: experimental analysis in a laboratory flume. *Advances in Water Resources* **81**, 128–141. doi:10.1016/j.advwatres.2015.01.005.

Termini, D. 2015b Flexible vegetation behavior and effects on flow conveyance: experimental observations. *International Journal of River Basin Management* **13** (4), 401–411. doi:10.1080/15715124.2015.1012519.

Termini, D. & Piraino, M. 2011 Experimental analysis of cross-sectional flow motion in a large amplitude meandering bend. *Earth Surface Processes and Landforms* **36** (2), 244–256.

Whiting, P. J. & Dietrich, W. E. 1990 Boundary shear stress and roughness over mobile alluvial beds. *Journal of Hydraulic Engineering* **116** (12), 1495–1511.

Xia, R. 1997 Relation between mean and maximum velocities in a natural river. *Journal of Hydraulic Engineering* **123** (8), 720–723.

Yalin, M. S. 1992 *River Mechanics*. Pergamon Press, Oxford, UK.

Yalin, M. S. & Da Silva, A. M. 2001 *Fluvial Processes*. IAHR Monograph, Delft, The Netherlands.

First received 13 April 2016; accepted in revised form 21 September 2016. Available online 5 December 2016